JOURNAL OF VIROLOGY, Oct. 2007, p. 10849–10860 Vol. 81, No. 20
0022-538X/07/$08.00+0 doi:10.1128/JVI.01151-07

West Nile Virus Infection Activates the Unfolded Protein Response, Leading to CHOP Induction and Apoptosis▽

Guruprasad R. Medigeshi,[1]* Alissa M. Lancaster,[1] Alec J. Hirsch,[1] Thomas Briese,[2] W. Ian Lipkin,[2] Victor DeFilippis,[1] Klaus Früh,[1] Peter W. Mason,[3] Janko Nikolich-Zugich,[1] and Jay A. Nelson[1]

Vaccine and Gene Therapy Institute, Oregon Health & Science University, 505 N.W. 185th Avenue, Beaverton, Oregon 97006[1]; Jerome L. and Dawn Greene Infectious Disease Laboratory, Mailman School of Public Health of Columbia University, 722 West 168th Street, 18th Floor, New York, New York 10032[2]; and 3.206B Mary Moody Northen Pavilion, Department of Pathology and Sealy Center for Vaccine Development, University of Texas Medical Branch, 301 University Boulevard, Galveston, Texas 77555-0436[3]

Received 25 May 2007/Accepted 24 July 2007

West Nile virus (WNV)-mediated neuronal death is a hallmark of WNV meningitis and encephalitis. However, the mechanisms of WNV-induced neuronal damage are not well understood. We investigated WNV neuropathogenesis by using human neuroblastoma cells and primary rat hippocampal neurons. We observed that WNV activates multiple unfolded protein response (UPR) pathways, leading to transcriptional and translational induction of UPR target genes. We evaluated the role of the three major UPR pathways, namely, inositol-requiring enzyme 1-dependent splicing of X box binding protein 1 (XBP1) mRNA, activation of activating transcription factor 6 (ATF6), and protein kinase R-like endoplasmic reticulum (ER) kinase-dependent eukaryotic initiation factor 2α (eIF2α) phosphorylation, in WNV-infected cells. We show that XBP1 is nonessential or can be replaced by other UPR pathways in WNV replication. ATF6 was rapidly degraded by proteasomes, consistent with induction of ER stress by WNV. We further observed a transient phosphorylation of eIF2α and induction of the proapoptotic cyclic AMP response element-binding transcription factor homologous protein (CHOP). WNV-infected cells exhibited a number of apoptotic phenotypes, such as (i) induction of growth arrest and DNA damage-inducible gene 34, (ii) activation of caspase-3, and (iii) cleavage of poly(ADP-ribose) polymerase. The expression of WNV nonstructural proteins alone was sufficient to induce CHOP expression. Importantly, WNV grew to significantly higher viral titers in *chop*$^{-/-}$ mouse embryonic fibroblasts (MEFs) than in wild-type MEFs, suggesting that CHOP-dependent premature cell death represents a host defense mechanism to limit viral replication that might also be responsible for the widespread neuronal loss observed in WNV-infected neuronal tissue.

West Nile virus (WNV) is a neurotropic virus that has reemerged as a pathogen of serious concern to the U.S. population, accounting for more than 20,000 reported human cases since the 1999 outbreak in New York (21, 40). Forty percent of the reported WNV-infected patients have neurological disease manifest as meningitis, encephalitis, and poliomyelitis. Immunocompromised and aged individuals are especially vulnerable to WNV infection. WNV belongs to the *Flaviviridae* family, which includes dengue virus, Japanese encephalitis virus (JEV), yellow fever virus, and the more distantly related hepatitis C virus (HCV), all of which are global health threats. The flaviviruses are characterized by a single-stranded positive-sense RNA genome of approximately 11,000 nucleotides that encodes a single polyprotein. The polyprotein is cleaved by host and viral proteases into three structural (capsid [C], membrane [M], and envelope [E]) and seven nonstructural (NS1, -2A, -2B, -3, -4A, -4B, and -5) proteins (21, 40).

Translation of the WNV polyprotein is associated with the endoplasmic reticulum (ER) membranes, and the ER is also the site of viral encapsidation and envelopment. Therefore, it is likely that WNV infection imposes a tremendous protein load on the ER, leading to perturbation of ER homeostasis. The unfolded protein response (UPR) is an ER-mediated response to the accumulation of large amounts of unfolded or misfolded proteins in the ER (12, 42). Induction of the UPR facilitates the recovery of the stressed ER by upregulating the expression of the protein folding machinery, such as the ER chaperones immunoglobulin heavy chain binding protein (BiP) and protein disulfide isomerase (PDI). Additionally, the UPR enhances the ER-assisted degradation (ERAD) of misfolded proteins. The UPR is mediated by the sequential and concerted activation of three key players, namely, protein kinase R (PKR)-like ER kinase (PERK), activating transcription factor 6 (ATF6), and inositol-requiring enzyme 1 (IRE1), whose functions are regulated by BiP (Fig. 1). Activation of PERK leads to phosphorylation of eukaryotic initiation factor 2α (eIF2α), resulting in the inhibition of protein translation (13). However, proteins such as ATF4 can bypass the translation inhibition and induce the expression of genes that help the ER to cope with the stress (28). ER stress leads to the translocation of ATF6, a bZIP family transcription factor, to the Golgi apparatus, where ATF6 is activated by limited proteolysis (5, 57). The cleaved N-terminal fragment of ATF6 is transported

* Corresponding author. Mailing address: Vaccine and Gene Therapy Institute, Oregon Health & Science University, 505 N.W. 185th Avenue, Beaverton, OR 97006. Phone: (503) 494-2434. Fax: (503) 494-6862. E-mail: medigesh@ohsu.edu.

▽ Published ahead of print on 8 August 2007.

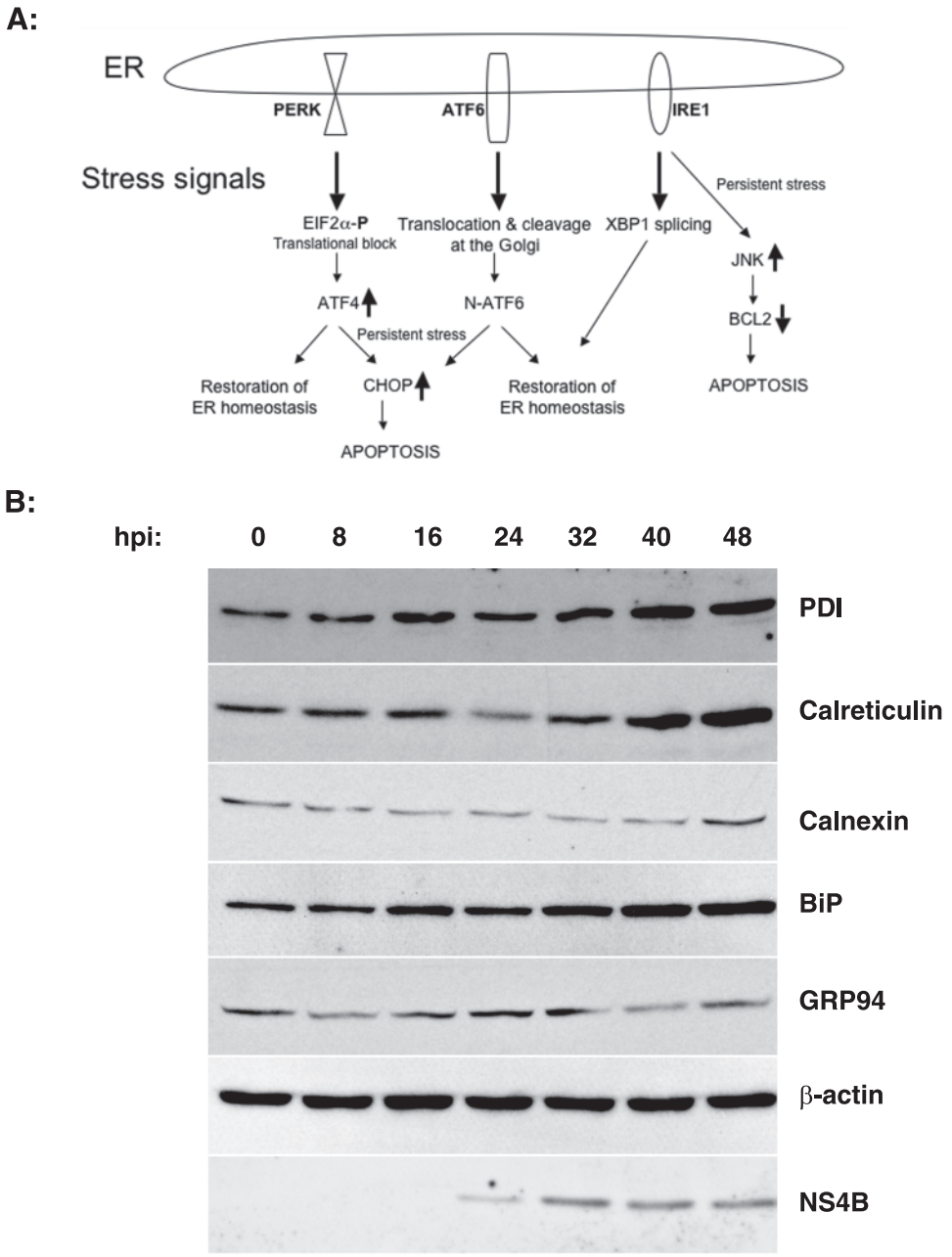

FIG. 1. WNV induces the expression of ER chaperones. (A) Schematic representation of the three arms of the mammalian UPR pathways. PERK, ATF6, and IRE1 regulate ER homeostasis by promoting prosurvival signals. Under prolonged ER stress, these proteins initiate apoptotic pathways to eliminate sick cells. See the introduction for a detailed description. (B) SK-N-MC cells were infected with WNV (MOI, 10), and lysates were harvested at the indicated times p.i. and analyzed by Western blotting for the indicated ER chaperones, β-actin, and WNV NS4B.

to the nucleus, where it activates the transcription of genes with ER stress response elements (ERSEs), which include ER chaperones and X box binding protein 1 (XBP1) (60). Finally, activation of IRE1, which consists of a serine-threonine kinase domain and an endoribonuclease domain, leads to splicing of the *xbp1* mRNA (excision of a 26-nucleotide intron), resulting in the expression of the XBP1s protein. XBP1s acts as a transcription factor, regulating the expression of ER chaperones and other genes that function to terminate the UPR by negative feedback inhibition of PERK (3, 25).

The UPR is a prosurvival signal that restores ER homeostasis by promoting either proper folding or degradation of accumulated misfolded proteins in the ER. However, in situations such as viral infections, ER stress is persistent and switches the UPR from being prosurvival to proapoptotic (47). Under these conditions, the PERK and IRE1 arms of the UPR suppress the activity of antiapoptotic proteins and induce the expression of proapoptotic proteins (53). ATF4 (induced by PERK activation) induces the expression of cyclic AMP (cAMP) response element-binding transcription factor homologous protein (CHOP; also

known as growth arrest and DNA damage-inducible gene 153 [GADD153]), which promotes apoptotic cell death (28). The proapoptotic action of IRE1 is mediated by the activation of the c-Jun N-terminal kinase (JNK), which promotes apoptosis by suppressing the activity of antiapoptotic Bcl-2 family proteins (7, 33, 58).

Flaviviruses have been shown to activate one or more UPR pathways. JEV induces the expression of CHOP, and both JEV and dengue virus induce splicing of *xbp1* (46, 61). HCV has been shown to activate IRE1, inhibit XBP1s activity, and block eIF2α phosphorylation (4, 48–50). Although these viruses differentially affect UPR pathways, a clear understanding of how flaviviruses such as WNV modulate all three arms of the UPR and the importance of this modulation in viral pathogenesis is lacking. In this study, we show that WNV-mediated ER stress affects the three UPR pathways differentially during the course of infection and provide evidence supporting an important role for CHOP-mediated apoptosis in limiting WNV growth. Our results provide insights into the cellular response to WNV infection and the molecular mechanisms of WNV pathogenesis.

MATERIALS AND METHODS

Cells, cell culture, and virus. SK-N-MC neuroblastoma cells were cultured in Dulbecco's modified Eagle's medium containing 10% fetal bovine serum, penicillin, streptomycin, and glutamine. HEK293T cells were cultured in minimal essential medium containing 10% fetal bovine serum, penicillin, streptomycin, and glutamine. *xbp1*$^{-/-}$ and *xbp1*$^{+/+}$ cells were obtained from Laurie Glimcher and grown as described previously (24). *chop*$^{-/-}$ cells were obtained from David Ron and cultured as described previously (63). The WNV strain used in this study has been described before (56). Viral stocks and infection and plaque assays were as described previously (15). In some experiments, viruses from WNV-infected mosquito cell (C6/36) supernatants were used. WNV replicons were packaged into virus-like particles (VLPs) by using a cell line persistently expressing a Venezuelan equine encephalitis virus replicon encoding the WNV structural proteins (10). To obtain high-titer WNV VLPs, we utilized a WNV replicon (WNR-CNS1-5) containing a full capsid-encoding region, since this replicon has been shown to produce high-titer VLP preparations (10; unpublished data). Rat hippocampal neurons were isolated and cultured in Gary Banker's laboratory as described previously (18).

Plasmid constructs and transfection. A plasmid encoding the structural region of WNV (pEF1-WNVstr) was constructed as follows. An infectious WNV clone (pFL-WNV) obtained from Pei-Yong Shi (44) was used as a template to amplify the region encoding the structural proteins (C-prM-E), using the forward primer 5′-ATCTCAGGTACCATGTCTAAGAAACC-3′ and the reverse primer 5′-TA GGATCCATTGATGCCCATCCAC-3′. The PCR product was cloned into the pcr2.1 vector (Invitrogen). A positive clone was cut with KpnI-BamHI, and the released insert was ligated into KpnI-BamHI sites of pEF1-mycHisB (Invitrogen). A stop codon at the end of the protein coding sequence in the vector abrogates the expression of tags at the C terminus. A positive clone verified by sequencing was used for transfections.

Transfection. HEK293T cells were transfected with the indicated plasmids in suspension, using the FuGENE6 transfection reagent (Roche Diagnostics) according to the manufacturer's instructions. At 16 to 24 h posttransfection, cells were infected (in the case of ATF6 transfections) with WNV as described above. Samples were processed at 24 and 48 h postinfection (p.i.) for Western blots or for RNA preparation as described below.

The pCMV-3xFLAG-ATF6 plasmid was a kind gift from Ron Prywes (43). For MG115 treatment, cells were treated at 36 h p.i. with dimethyl sulfoxide or 50 μM MG115 (Sigma) for 4 h, and cell lysates were prepared as described below for Western analysis.

Antibodies. The following commercial antibodies were used in this study: monoclonal anti-BiP (BD Biosciences), monoclonal anti-calnexin (Affinity Bioreagents), monoclonal anti-glucose response protein 94 (anti-GRP94), polyclonal anti-PDI (both from Stressgen), polyclonal anti-CHOP (Santa Cruz Biotechnology), anti-FLAG (M2; Sigma), anti-eIF2α, anti-phospho-eIF2α, anti-caspase 3, and anti-poly(ADP-ribose) polymerase (anti-PARP; Cell Signaling).

NS3, NS4B, and NS5 antisera. Monospecific polyclonal rabbit antisera were raised against WNV proteins NS3, NS4B, and NS5. Coding sequences were amplified by PCR from WNV-NY99 RNA and cloned into the NdeI and BamHI restriction sites of pET-15B (Novagen) expression plasmid vectors to generate N-terminally histidine-tagged proteins. Insert-bearing plasmid DNAs were transformed into *Escherichia coli* BL21(DE3) cells for isopropyl-β-D-galactopyranoside (IPTG)-induced expression of recombinant NS3-His, NS4B-His, and NS5-His. Cells were disrupted by sonication in IMAC buffer (500 mM NaCl, 10% glycerol, 0.2% Triton X-100, 20 mM Tris-HCl, pH 8) containing 5 mM imidazole (NS3-His) or 0.1 sodium phosphate (pH 8)–8 M urea containing 5 mM imidazole (NS4B-His and NS5-His). Proteins were purified on nickel-agarose (QIAGEN), using IMAC buffer containing 25 mM imidazole (NS3-His) or 0.1 sodium phosphate (pH 8)–8 M urea containing 25 mM imidazole (NS4B-His and NS5-His) for washing and IMAC buffer containing 250 mM imidazole (NS3-His) or 0.1 sodium phosphate (pH 8)–8 M urea containing 250 mM imidazole (NS4B-His and NS5-His) for elution. Purified proteins were adjusted to 1 to 1.5 μg/μl in phosphate-buffered saline (PBS) (NS3) or PBS–8 M urea (NS4B and NS5). Rabbits were immunized with 0.5 mg purified protein per injection, applying three consecutive injections at 3-week intervals, using Freund's complete (day 1) or incomplete (days 21 and 42) adjuvant.

Cell lysate preparation and Western blotting. Cell lysates were prepared by washing cells on ice with PBS twice and scraping them into lysis buffer containing 50 mM Tris-HCl, pH 8, 150 mM sodium chloride, 1% NP-40, 0.25% sodium deoxycholate, 1 mM EDTA, and protease inhibitor cocktail containing aprotinin, leupeptin, and pepstatin. For phospho-eIF2α Western blots, 1 mM sodium fluoride, 1 mM sodium orthovanadate, 20 mM β-glycerophosphate, and 20 mM sodium pyrophosphate were added to the above lysis buffer. After 10 min of incubation on ice, samples were centrifuged at 13,000 × *g* for 10 min at 4°C, and supernatants were used for protein estimation by the method of Bradford (Bio-Rad). Lysates (25 to 50 μg) were loaded into a sodium dodecyl sulfate-polyacrylamide gel, transferred to a polyvinylidene difluoride membrane (Immobilon-Millipore), and probed with appropriate antibodies followed by horseradish peroxidase-conjugated anti-rabbit or anti-mouse antibodies (GE Healthcare). Blots were visualized with the Supersignal West Pico chemiluminescent substrate (Pierce) according to the manufacturer's protocol. Signal intensities were quantitated by IPLab Gel H software (Analytics Corp.).

Xbp1 splicing. Activation of Ire1p was determined by measuring the splicing of its substrate, the mRNA encoding the XBP1 transcription factor. RNA was harvested using TRIzol reagent per the manufacturer's instructions (Invitrogen). Total RNA was treated with DNase I (DNase-free; Ambion) before the synthesis of cDNA by random hexamers and Superscript III (Invitrogen). To amplify *xbp1* mRNA, PCR was performed for 30 cycles (94°C for 30 s, 58°C for 30 s, and 72°C for 1 min [10 min in the final cycle]), using the primers 5′-CTGGAAAGCAAG TGGTAGA-3′ and 5′-CTGGGTCCTTCTGGGTAGAC-3′ with Platinum *Taq* DNA polymerase (Invitrogen). Fragments of 398 bp and 424 bp, representing spliced (XBP1s) and unspliced XBP1, respectively, were documented after staining 2% agarose gels with ethidium bromide and viewing them by UV illumination.

qRT-PCR. CHOP-specific quantitative real-time reverse transcription-PCR (qRT-PCR) was performed by both primer-probe and SYBR green-based methods.

(i) Primer-probe set. Cells were collected in 0.5 to 1 ml TRIzol reagent (Invitrogen), and RNAs were prepared according to the manufacturer's instructions. One hundred nanograms of RNA was used to determine WNV copy numbers by one-step RT-PCR analysis (Applied Biosystems). The WNV primers and probe used have been described before (2). Genome copy numbers were normalized to β-actin values determined in parallel using Taqman gene expression assay endogenous control primer-probe sets (Applied Biosystems). Relative CHOP mRNA levels were measured by qRT-PCR, using primer-probe sets from the Applied Biosystems inventory (assay Hs99999172_m1).

(ii) SYBR green method. For qRT-PCR of CHOP from primary rat neurons, RNAs were harvested as described above and total RNA was treated with DNase I (DNase-free; Ambion) before synthesis of cDNA by random hexamers and Superscript III (Invitrogen). Primers were selected by using Primer Express software (Applied Biosystems). Relative levels of the following mRNAs were measured by qRT-PCRs using the following primers: rat CHOP forward primer, 5′-GGAAAGTGGCACAGCTTGCT-3′; rat CHOP reverse primer, 5′-CTGGT CAGGCGCTCGATT-3′; L32 ribosomal protein forward primer, 5′-GAAGAT TCAAGGGCCAGATCC-3′; and L32 ribosomal protein reverse primer, 5′-GT GGACCAGAAACTTCCGGA-3′. For qRT-PCR of human samples, the primer sets shown in Table 1 were used to amplify the indicated mRNAs.

Reactions were performed using SYBR green PCR core reagents. Relative expression values between mock and infected samples at each time point were calculated by the comparative cycle threshold method as previously described (1a). Dissociation curves were done after each amplification run to control for

TABLE 1. Primers used to amplify mRNAs from human cell lysates

Gene	Primer sequence	
	5′ Primer	3′ Primer
CHOP	AGCTGGAACCTGAGGAGAGA	TGGATCAGTCTGGAAAAGCA
ATF6	CTTTTAGCCCGGGACTCTTT	TCAGCAAAGAGAGCAGAATCC
GADD34	GGAGGAAGAGAATCAAGCCA	TGGGGTCGGAGCCTGAAGAT
WNV	GGCGGTCCTGGGTGAAGTCAA	CTCCGATTGTGGTTGCTTCGT
β-Actin	CAGGGGAACCGCTCATTGCCAATGG	TCACCACACACTGTGCCCATCTACGA

primer dimers. Absolute standard curves were generated from a plasmid encoding the WNV NS1 or NS3 cDNA.

Statistical analysis. *P* values were obtained by two-tailed, unpaired Student's *t* test.

RESULTS

WNV infection leads to induction of ER chaperones. We investigated the modulation of the UPR by WNV in SK-N-MC neuroblastoma cells, which are susceptible to WNV infection, as shown previously (15). In order to determine if WNV infection elicits an ER stress response, cells were infected with WNV and the expression levels of the ER chaperones BiP, PDI, glucose response protein 94 (GRP94), calnexin, and calreticulin were monitored over the course of infection by Western blot analysis. As shown in Fig. 1B, ER chaperones were induced upon WNV infection, starting at 16 h p.i., and at 48 h p.i. we observed two- to threefold increases in BiP, PDI, calreticulin, and calnexin protein levels, with a modest increase in GRP94 levels at 24 and 32 h p.i. The kinetics of chaperone induction coincided with the expression of WNV protein NS4B, suggesting that the viral protein load in the ER induces ER stress and the upregulation of ER chaperones. β-Actin levels remain unchanged during the course of infection, indicating that the induction is chaperone specific and not due to global upregulation of protein translation.

WNV activates IRE1, leading to XBP1 splicing. Because induction of chaperones is a characteristic feature of the activation of the UPR, we investigated the activation of all three arms of the UPR in WNV-infected cells. Activation of the IRE1 endoribonuclease leads to mRNA splicing of the transcription factor XBP1 by removing a 26-bp intron from the *xbp1* transcript, which generates a frameshift in the XBP1 open reading frame. This results in the expression of the active form of the protein, XBP1s, which acts as a transcription factor. XBP1s is involved in the transcriptional induction of a subset of UPR target genes and also of the genes involved in ERAD pathways (60). Analysis of *xbp1* splicing in WNV-infected cells revealed that splicing occurred by 24 h p.i. and that by 45 h p.i. most of the *xbp1* mRNA was spliced (Fig. 2A). The kinetics of splicing corresponded with the increase in WNV titers in culture supernatants, suggesting that the activation of IRE1 is due to an increasing viral load in the ER (Fig. 2A). XBP1 has been shown to be essential for the expression of only a subset of UPR target genes (24). In order to determine if XBP1 plays an essential role in WNV replication, we performed growth curve experiments with mouse embryonic fibroblasts (MEFs) derived from $xbp1^{-/-}$ and $xbp1^{+/+}$ embryos. As shown in Fig. 2B, the lack of *xbp1* had no effect on the growth of WNV, indicating that XBP1 is dispensable for WNV growth.

WNV infection leads to degradation of ATF6. ATF6 is a bZIP family transcription factor associated with the ER. Upon induction of ER stress, ATF6 transits to the Golgi complex, where resident proteases cleave ATF6 at the N terminus. The N-terminal fragment is translocated into the nucleus, where it upregulates the expression of various chaperones, including BiP (5). We analyzed the activation of ATF6 in WNV-infected cells by transient transfection of 293T cells with FLAG epitope-tagged ATF6 (43), followed by infection with WNV. Cleavage of ATF6 was analyzed by Western blotting of the lysates from infected cells. We observed that WNV-infected lysates had much less ATF6 than did uninfected controls (Fig. 2C). Additionally, we analyzed endogenous *atf6* mRNA levels in WNV-infected SK-N-MC cells and did not observe any changes, indicating that the difference occurs at a posttranscriptional step (data not shown). Previous studies have shown rapid degradation of ATF6 upon ER stress, in a proteasome-dependent manner (16). To confirm if ATF6 degradation in WNV infection occurs in a similar fashion, WNV-infected cells were treated at 36 h p.i. with the proteasomal inhibitor MG115 for 4 h, and cell lysates were analyzed by Western blotting for a reduction of ATF6 degradation. As expected, MG115 treatment by itself caused ER stress and led to some degree of cleavage of ATF6 (Fig. 2C). Nevertheless, we observed a partial rescue (about 30% increase) of ATF6 levels in lysates from MG115-treated cells (Fig. 2C). These results suggest that the ER stress in WNV-infected cells causes rapid degradation of ATF6 by the proteasome.

WNV infection leads to eIF2α phosphorylation. Activation of PERK leads to phosphorylation of eIF2α, resulting in global inhibition of protein translation (13). We analyzed eIF2α phosphorylation in lysates from WNV-infected cells as a measure of PERK activation by Western blotting. As a positive control, we used cell lysates treated with thapsigargin, which perturbs ER calcium levels and causes ER stress. As shown in Fig. 3A, eIF2α was phosphorylated upon WNV infection at 24 h p.i.; however, this effect was not sustained, as phospho-eIF2α signals were back to basal levels at later stages of infection (48 h p.i.). The eIF2α phosphorylation induced by WNV was similar to that observed in response to thapsigargin (Fig. 3A), indicating that WNV is a highly potent ER stressor. The total levels of eIF2α in the lysates over the course of infection were unchanged. These results suggest that WNV infection also activates the PERK arm of the UPR but that eIF2α phosphorylation is overcome by WNV at later stages in the infection.

WNV infection induces proapoptotic CHOP expression. WNV infection has been shown to induce apoptosis in neurons and various other cell types (41, 45). PERK activation and eIF2α phosphorylation lead to the activation of ATF4, which

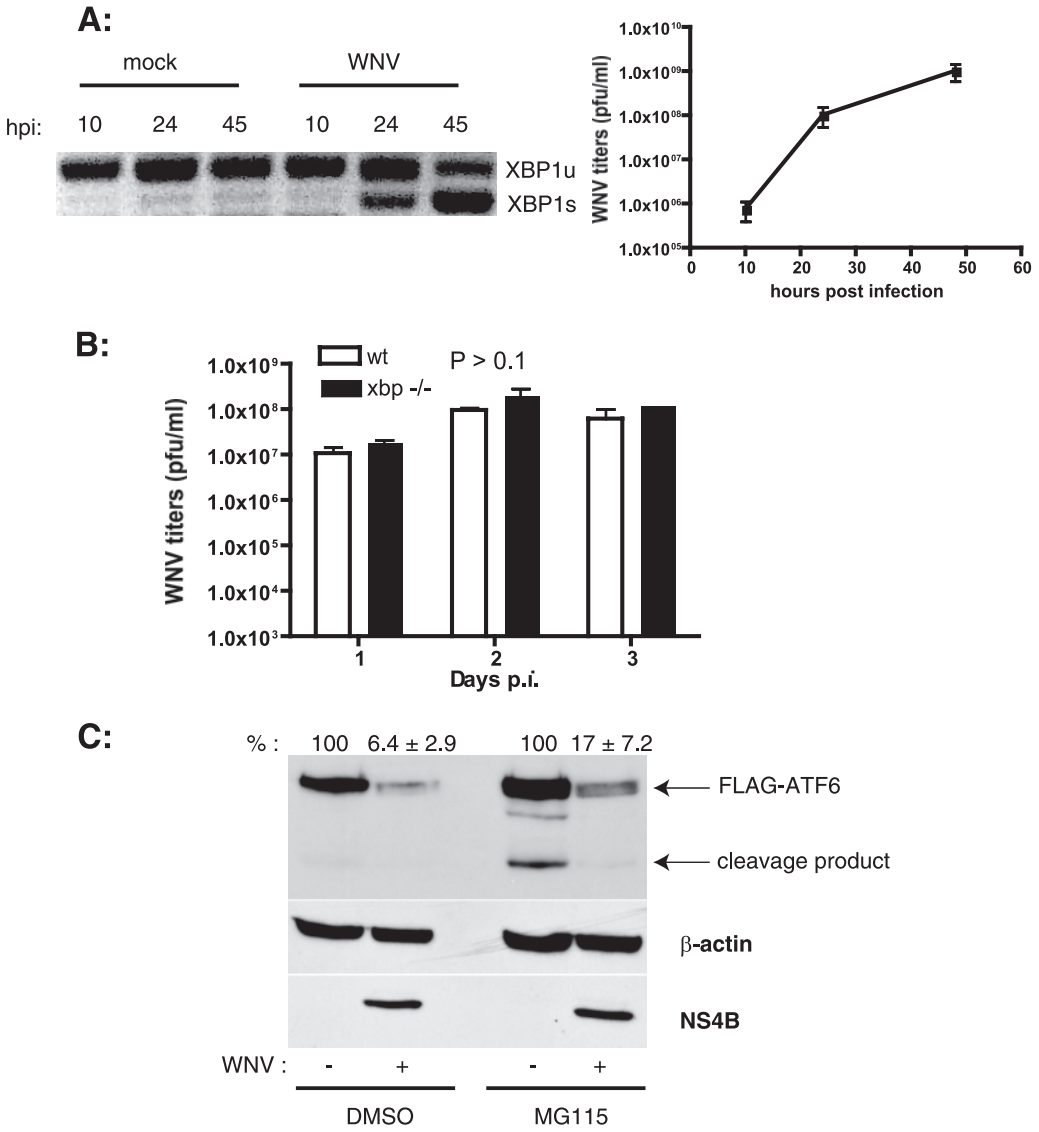

FIG. 2. WNV infection induces *xbp1* splicing and ATF6 degradation. (A) SK-N-MC cells were infected with WNV (MOI, 10), and total RNA was isolated from cells at the indicated times p.i. *xbp1* splicing was analyzed by PCR as described in Materials and Methods. Unspliced (*xbp1u*) and spliced (*xbp1s*) forms are shown. WNV titers in the culture supernatants were determined by plaque assay on Vero cells. Results are representative of two independent experiments. Data are means ± standard deviations (SD). (B) Wild-type (wt) and *xbp1*$^{-/-}$ cells were infected with WNV at an MOI of 3. Supernatants were collected on the indicated days p.i., and WNV titers were determined by plaque assay on Vero cells. Three independent experiments were performed with duplicate samples. Data are means ± SD. (C) HEK293T cells were transfected with a plasmid expressing 3× FLAG-ATF6 followed by infection with WNV at an MOI of 5. At 36 h p.i., cells were treated with dimethyl sulfoxide or 50 μM MG115 for 4 h, and cell lysates were analyzed by Western blotting using anti-FLAG, anti-β-actin, and anti-WNV NS4B antibodies. ATF6 expression levels (averages ± SD) from two independent experiments are indicated.

upregulates genes involved in restoring ER homeostasis. However, under persistent ER stress, ATF4 induces the expression of CHOP, which initiates apoptosis (28). To determine if CHOP expression is induced by WNV, we analyzed the levels of *chop* mRNA by qRT-PCR and of CHOP protein by Western blotting with RNA samples and cell lysates prepared from WNV-infected cells. We found that CHOP mRNA levels were persistently induced by WNV at 24 and 48 h p.i. (Fig. 3B). CHOP was barely detectable in the lysates under normal conditions. We observed an induction of CHOP protein levels in WNV-infected cell lysates (Fig. 3C), confirming the qRT-PCR results. These results suggest a possible mechanistic link between WNV-induced apoptosis and CHOP induction.

WNV induces eIF2α phosphorylation and CHOP in primary neurons. The most severe cases of WNV disease involve viral invasion of the central nervous system and subsequent encephalitis and/or meningitis. Pathology studies of WNV-infected patients and animals have shown a rapid loss of neurons by apoptosis (1, 11, 38, 39, 41, 45). Our results with neuroblastoma cells implicate a potential role for UPR-mediated apoptosis in neuronal death. We used primary rat hippocampal neuronal/glial cultures as a model to understand the mechanism of neuronal ap-

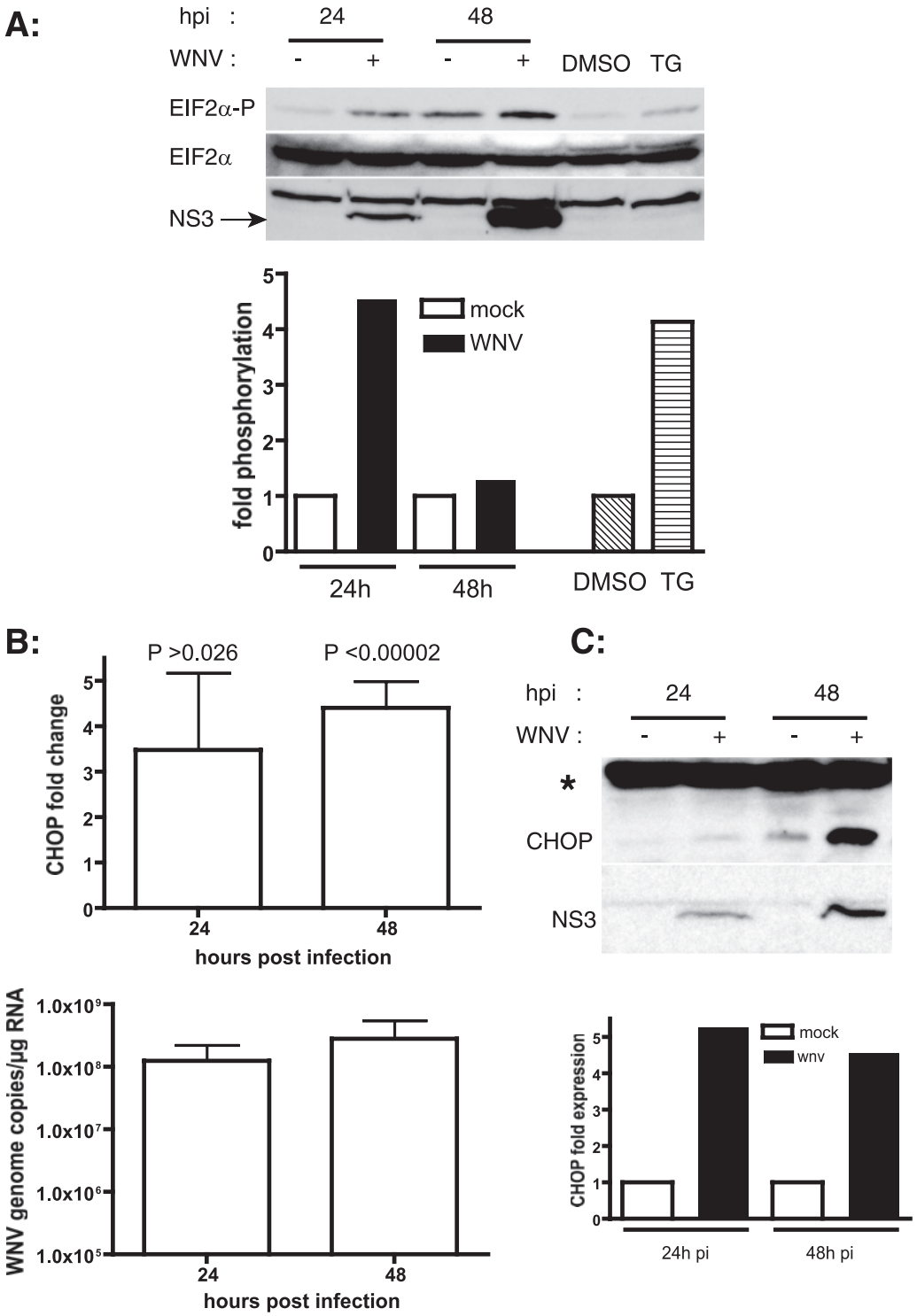

FIG. 3. WNV activates eIF2α kinases and induces CHOP expression. (A) SK-N-MC cells were infected with WNV (MOI, 10), and cell lysates were prepared at the indicated times p.i. and analyzed by Western blotting to detect phospho-eIF2α and total eIF2α. WNV infection was confirmed by probing the blots with WNV NS3 antibodies. Signal intensities were quantitated, and phospho-eIF2α signals were normalized to total eIF2α levels. Cell lysates treated with 1 μM thapsigargin (TG) served as a positive control for ER stress-induced eIF2α phosphorylation. (B) SK-N-MC cells were infected with WNV (MOI, 10), and total RNA was prepared from cells at the indicated times p.i. *chop* mRNA was quantitated by real-time RT-PCR. WNV NS1 was quantitated from the same samples as a measure of infection. *chop* message levels were normalized to β-actin mRNA levels, and *x*-fold changes were calculated as described in Materials and Methods. Data represent averages for four independent experiments performed with duplicate samples. Data are means ± SD. (C) Cell lysates prepared from WNV-infected SK-N-MC cells at 24 and 48 h p.i. were analyzed by Western blotting for CHOP expression. A nonspecific protein (*) served as a loading control. WNV infection was confirmed by Western blotting against WNV NS3.

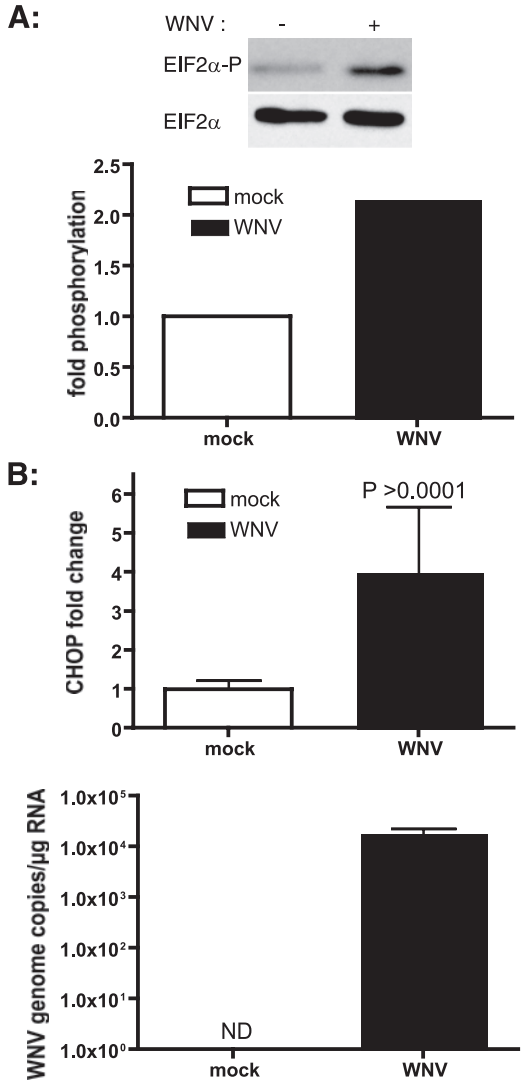

FIG. 4. WNV induces eIF2α phosphorylation and CHOP in primary rat hippocampal neurons. (A) One-week-old primary rat neurons were infected with WNV at an MOI of 10. At 24 h p.i., lysates were prepared and analyzed for phospho-eIF2α and total eIF2α by Western blotting. (B) Total RNA was isolated from WNV-infected neurons at 24 h p.i., and *chop* mRNA levels were quantitated by real-time RT-PCR. The *chop* message was normalized to the ribosomal protein L32 message, and *x*-fold changes were calculated as described in Materials and Methods. WNV infection was verified by WNV NS1 amplification from the samples. ND, not detected. Data represent three independent experiments and are means ± SD.

optosis. Cultures were infected with WNV, and subsequently, eIF2α phosphorylation was monitored in the lysates. We observed a twofold increase in phospho-eIF2α levels at 24 h p.i. (Fig. 4A), while the total level of eIF2α remained unchanged. We further isolated RNAs from WNV-infected neurons, and induction of *chop* was analyzed by qRT-PCR. As shown in Fig. 4B, we saw a four- to fivefold increase in the *chop* mRNA level relative to that in uninfected samples. These results suggest a potential role for CHOP in WNV-induced neuronal apoptosis.

WNV induces expression of GADD34, activation of caspase 3, and PARP cleavage. CHOP promotes cell death by a dual mechanism, i.e., by activation of proapoptotic genes and by downregulation of antiapoptotic genes (30, 31, 35, 54). One of the downstream effectors of CHOP is GADD34, the regulatory subunit of the eIF2α-specific phosphatase complex (20, 34). GADD34 activity dephosphorylates eIF2α, relieving translation attenuation, promoting protein synthesis, and thereby aggravating the accumulation of unfolded and misfolded proteins in the ER. In order to further characterize the role of CHOP effectors such as GADD34 in WNV-mediated apoptosis, we examined the expression of GADD34 in WNV-infected cells. qRT-PCR analysis of RNAs from WNV-infected samples showed a persistent twofold induction of GADD34 compared to the level in uninfected samples (Fig. 5A). These results suggest that WNV upregulation of GADD34 counteracts eIF2α phosphorylation and relieves translation inhibition to facilitate the synthesis of viral proteins.

CHOP induction activates apoptotic pathways, culminating in cell death. ER stress-mediated apoptotic signals ultimately converge on caspase 3, which is the effector caspase activated by proteolytic cleavage. Caspase 3 has been shown to play a role in neuronal apoptosis in WNV-infected animals (41). We analyzed the activation of caspase 3 during the course of WNV infection in WNV-infected cell lysates. As shown in Fig. 5B, caspase 3 was activated at 48 h p.i., as observed by the appearance of 17-kDa cleavage fragments. We next looked at the proteolytic cleavage of PARP by caspases, which is another hallmark of apoptosis (23). Western blot analysis of WNV-infected lysates revealed PARP cleavage at 48 h p.i. (Fig. 5C), which correlated with the activation of caspase 3 (Fig. 5B). Taken together, our results indicate that the persistent activation of UPR pathways by WNV leads to the induction of apoptosis.

CHOP induction by WNV is mediated by NS proteins. WNV particle formation has been proposed to occur in close association with the ER membranes. Both structural and NS proteins could be responsible for activating the UPR, inducing the expression of CHOP, and promoting apoptosis. In order to identify the region of the WNV polyprotein responsible for CHOP induction, we investigated the involvement of structural and NS proteins in inducing CHOP expression. HEK293T cells were transfected with a plasmid encoding the WNV structural region (C, prM, and E) or infected with WNV or with WNV-derived VLPs expressing replicons encoding capsid and NS1 to -5 (WNR-CNS1-5) (10). Western blotting of E and NS5 from cell lysates revealed comparable expression levels between plasmid transfection and VLP infection. However, WNV-infected lysates had much higher levels of E and NS5 (Fig. 6A). *chop* expression was analyzed by qRT-PCR, as mentioned above. We observed a threefold induction of *chop* mRNA in WNV-infected samples (Fig. 6A). WNV structural proteins failed to induce *chop*, while the VLPs expressing NS proteins induced *chop* expression to levels almost similar to those for WNV. These results demonstrate that one or more NS proteins of WNV induce CHOP expression, leading to apoptosis.

CHOP-deficient cells release larger amounts of WNV. MEFs derived from *chop*$^{-/-}$ embryos provided further insights into the role of CHOP in ER stress-induced apoptosis. *chop*$^{-/-}$ cells have been shown to be partially resistant to apoptosis induced by ER stress (63). In order to determine if CHOP plays a role in WNV replication, we analyzed the growth of

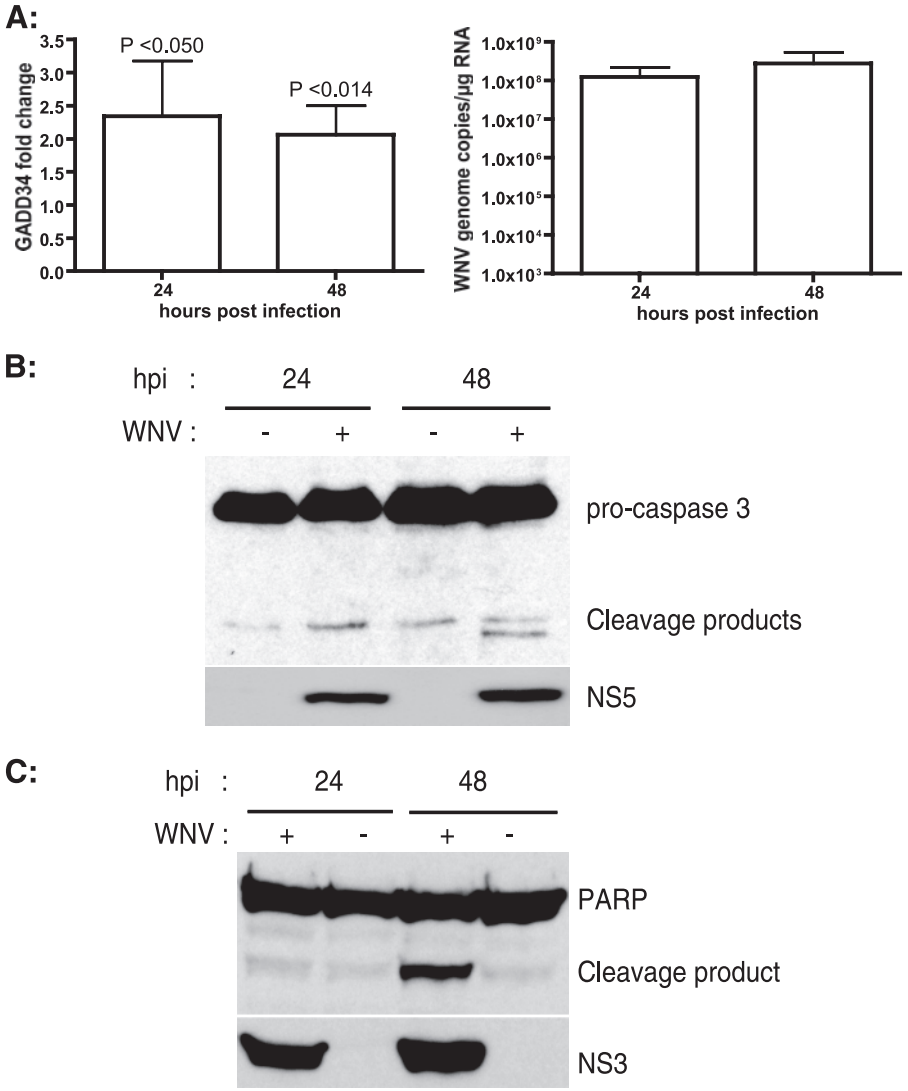

FIG. 5. WNV infection leads to apoptosis. (A) SK-N-MC cells were infected with WNV (MOI, 10), and total RNA was prepared from cells at the indicated times p.i. The GADD34 message was quantitated by real-time RT-PCR. WNV NS1 was quantitated from the same samples to verify infection. GADD34 message levels were normalized to β-actin levels, and *x*-fold changes were calculated as described in Materials and Methods. Data represent averages for four independent experiments performed with duplicate samples. Error bars represent SD. (B and C) SK-N-MC lysates isolated at 24 and 48 h post-WNV infection were analyzed by Western blotting for caspase 3, PARP, and WNV NS3/5.

WNV in wild-type and *chop*$^{-/-}$ MEFs. As shown in Fig. 6B, *chop*$^{-/-}$ MEFs supported robust WNV infection, leading to titers significantly higher than those in the wild-type MEFs at both 24 and 48 h p.i. Analysis of WNV protein levels showed significantly larger amounts of NS3 in lysates from *chop*$^{-/-}$ cells than in lysates from wild-type controls. These results suggest that CHOP-mediated apoptosis functions to control WNV replication in vitro and that this process may represent an important in vivo mechanism of control of WNV replication and pathogenesis as well.

DISCUSSION

In the current study, we have shown that WNV infection triggers the activation of all three arms of the UPR. In WNV-infected cells, we observed induction of the expression of the ER chaperones BiP, PDI, calreticulin, calnexin, and GRP94. BiP is the master regulator of the UPR pathways and regulates the activation of PERK, ATF6, and IRE1 (42). Overloading of the ER with unfolded or misfolded proteins results in the sequestration of BiP and in activation of the UPR. It is likely that in WNV-infected cells, the abundance of ER-localized viral proteins triggers this process. WNV infection activates IRE1, resulting in the splicing of *xbp1* mRNA. However, the growth of WNV is unchanged in *xbp1*$^{-/-}$ cells compared to that in wild-type cells, indicating that this arm of the UPR does not affect WNV replication or that its effects are redundant. XBP1 is essential for the expression of a subset of ER stress-responsive genes involved in ER biogenesis (24). Flavivirus replication is associated with extensive proliferation of intracellular membranes, which are, in part, derived from the ER. However, it is possible that other UPR pathways compensate

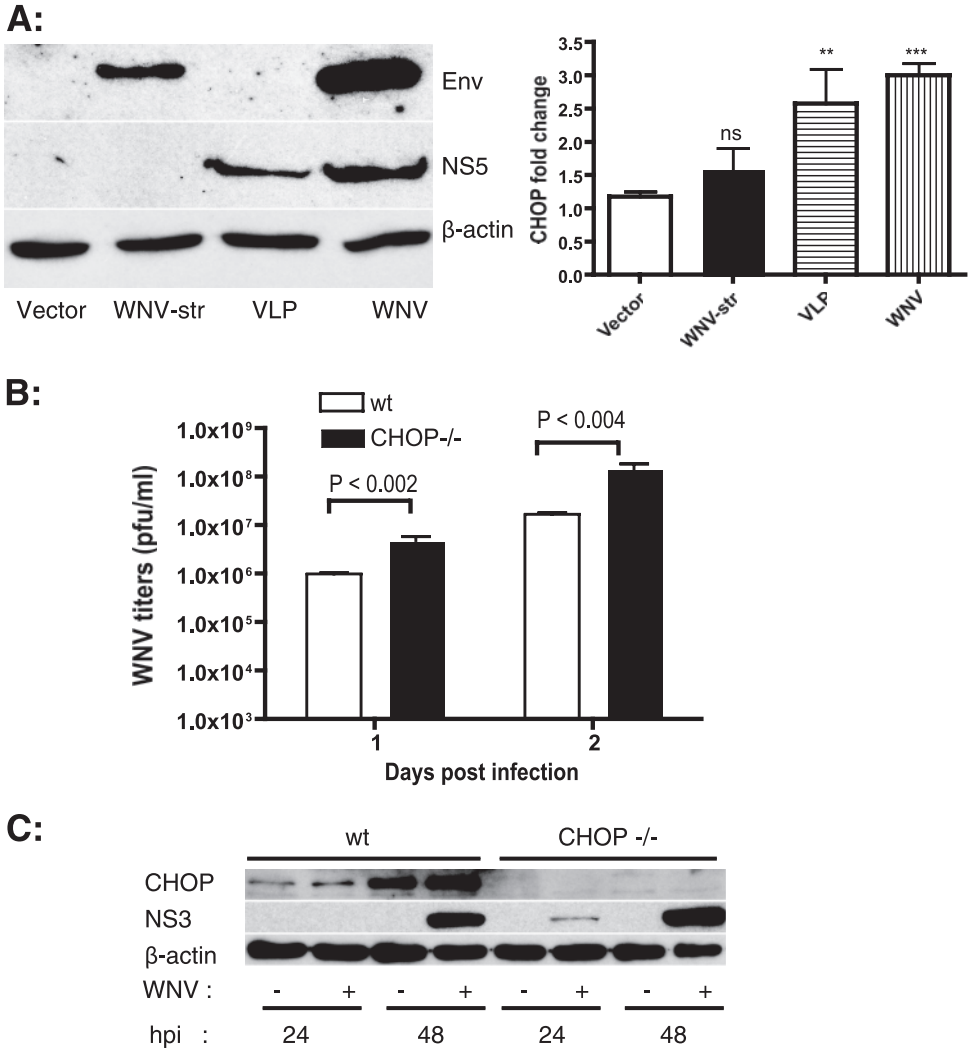

FIG. 6. WNV NS proteins induce CHOP expression and WNV growth in *chop*$^{-/-}$ MEFs. (A) HEK293T cells were transfected with the indicated plasmids or infected with VLPs or WNV. At 42 h posttransfection/infection, total RNA was isolated and *chop* mRNA levels were quantitated as mentioned above. Expression of WNV E and NS5 in the transfected/infected cell lysates was verified by Western blotting. β-Actin is shown as a loading control. (B) Wild-type (wt) and *chop*$^{-/-}$ MEFs were infected with WNV at an MOI of 1, and supernatants were collected at 24 and 48 h p.i. WNV titers were determined by plaque assay on Vero cells. Data representative of three independent experiments performed with triplicate values are shown. Data are means ± standard errors of the means. The respective *P* value for each sample compared with the vector alone is indicated as follows: ns, not significant ($P > 0.221$); **, $P < 0.037$; and ***, $P < 0.0009$. (C) Cell lysates isolated at 24 and 48 h p.i. from WNV-infected wild-type (wt) and *chop*$^{-/-}$ MEFs were analyzed by Western blotting for CHOP, WNV NS3, and β-actin.

for the absence of XBP1 in these cells. Our results are consistent with reports on other flaviviruses, such as JEV and dengue virus, where knockdown of XBP1 expression by small interfering RNA had minimal effects on viral growth (61). XBP1 is also involved in ERAD by the induction of ER degradation-enhancing α-mannosidase-like protein (EDEM) (52, 59). Interestingly, expression of the HCV replicon induces XBP1 splicing but inhibits XBP1s activity by targeting the protein for proteasomal degradation, thus blocking the induction of ERAD. We have not investigated whether or not WNV inhibits XBP1s activity. However, we show that ATF6 is rapidly degraded in a proteasome-dependent manner following WNV infection. ATF6 activation is upstream of IRE1 activation, and cleavage of ATF6 is required for the induction of XBP1 mRNA (25). Therefore, WNV and HCV may inhibit ERAD by acting on different proteins in the same pathway. There are no reports of viruses inducing ATF6 degradation so far, and whether WNV-mediated degradation of ATF6 results in the inhibition of ERAD by negative regulation of *xbp1* warrants further investigation.

WNV infection leads to transient phosphorylation of eIF2α, presumably via activation of PERK, in both SK-N-MC cells and primary rat hippocampal neurons. Furthermore, we showed that persistent ER stress due to WNV infection finally leads to the induction of the proapoptotic genes *chop* (*gadd153*) and *gadd34* and that WNV-infected cells exhibit caspase 3 activation and PARP cleavage, indicating that apoptosis of infected cells does indeed occur. The UPR often func-

tions as a prosurvival signal to promote the restoration of ER homeostasis. However, persistent stress inflicted upon the ER by viral proteins switches UPR signals from being prosurvival to prodeath by inducing the expression of genes involved in apoptosis. Induction of CHOP is observed following expression of the WNV NS, but not structural, proteins, demonstrating that one or more of these proteins is sufficient to trigger this process. WNV titers in *chop*$^{-/-}$ cells were significantly higher than those in wild-type MEFs, strongly suggesting that apoptosis functions to limit viral replication.

eIF2α phosphorylation by PERK plays a key role in the UPR by promoting translational shutoff to allow proper folding of unfolded and misfolded proteins accumulated in the ER (13). eIF2α is also phosphorylated by other kinases, such as the general control nondepressible 2 kinase and interferon-inducible PKR, which is activated by double-stranded RNA (8). However, there are no reports linking these kinases to ER stress. PKR-deficient MEFs do not show any defects in ER stress-induced translation inhibition, suggesting that PKR is not involved in the UPR (13). Additionally, a cytopathic strain of bovine viral diarrhea virus, a related member of the *Flaviviridae* family, has been shown to activate PERK and to induce eIF2α phosphorylation (17). Our studies are consistent with this observation and implicate PERK activation in eIF2α phosphorylation in both neuroblastoma cells and primary neurons. Nevertheless, PKR and general control nondepressible 2 kinase may also be involved in eIF2α phosphorylation at early stages of infection in response to viral RNA replication. Translation inhibition has a deleterious effect on viral growth, and viruses have been shown to overcome this inhibition by various mechanisms. For example, the herpes simplex virus-encoded protein ICP34.5 binds to a host serine/threonine phosphatase, protein phosphatase 1α, which dephosphorylates eIF2α, relieving translation inhibition (14). The human papillomavirus type 18 E6 oncoprotein has been shown to associate with GADD34, which facilitates translation recovery by dephosphorylating eIF2α (19). The HCV envelope protein E2 has been shown to inhibit PERK by direct binding (37). We show that transient phosphorylation of eIF2α in WNV-infected cells leads to persistent activation of the proapoptotic transcription factor CHOP. CHOP plays a critical role in ER stress-induced apoptosis, as demonstrated by the partial resistance of CHOP-deficient MEFs to apoptosis by chemical agents inducing ER stress (63). Numerous genes have been identified as downstream targets of CHOP, one of which is *gadd34* (54). GADD34 has been shown to recruit PP1 to dephosphorylate eIF2α, thereby relieving translation attenuation and increasing the client protein load in the ER, leading to apoptosis (34). Our data suggest that WNV overcomes the host translation inhibition response by upregulating GADD34 activity via chop induction.

A number of studies have reported upregulation of the UPR and other markers of ER stress, including CHOP, in neurodegenerative disorders, such as Alzheimer's disease, Parkinson's disease, and spinocerebellar ataxias (29, 35, 62). Increased levels of CHOP, JNK, and caspase 12 activation have been observed in neurons undergoing apoptosis due to perturbations in ER calcium levels (35, 51). CHOP mRNA is induced in the rat hippocampus subjected to global cerebral ischemia, which occurs due to depletion of calcium stores from the ER (22, 36). Induction of CHOP expression has been implicated in the apoptosis of Purkinje neurons infected with Borna disease virus (55). A number of neurovirulent viruses, including JEV, have been shown to modulate CHOP expression, indicating an important role for CHOP-mediated apoptosis in viral pathogenesis (9, 26, 27, 32, 46). Neurological manifestations of WNV fever include a rapid loss of motor neurons, a primary cause of WNV encephalitis and paralysis (6). Neuronal loss is one of the characteristic features observed in brains and spinal cords of WNV-infected mice and in brain tissue autopsies of infected humans (1, 11, 38, 39, 45). Previous studies have shown that WNV infection causes apoptosis in the neurons, but the underlying mechanism remained unclear. Our results implicate a crucial role for CHOP in WNV-induced apoptosis of both SK-N-MC cells and primary neurons. Apoptosis has opposing effects on viral pathogenesis by either preventing viral dissemination due to the death of infected cells or promoting viral spread by release of the progeny virus from cells undergoing apoptosis. Apoptosis in nonrenewable cell populations, such as neurons, has serious consequences for the host. CHOP induction leads to a number of changes in cellular homeostasis, culminating in apoptosis. CHOP induction leads to transcriptional downregulation of the proapoptotic gene *bcl2*. It has been reported that overexpression of CHOP results in thiol depletion, which results in redox imbalance and increased production of reactive oxygen species (31). *chop*$^{-/-}$ cells are probably protected from these deleterious effects, and this could enable robust WNV replication in these cells, as observed in our study. Characterizing WNV growth and pathogenesis in *chop*$^{-/-}$ mice should help us to further understand the exact role of CHOP in WNV spread and disease in various organs. Furthermore, identification of the specific WNV protein(s) involved in CHOP induction will provide insights into the mechanistic details of CHOP-mediated apoptosis in WNV infection. Our study provides a comprehensive picture of the activation of UPR pathways in WNV infection. Understanding the mechanism of WNV interactions with the UPR pathways will help to elucidate the positive and negative consequences of these pathways on WNV pathogenesis and ultimately provide clues to the design of new therapies for flavivirus-induced disease.

ACKNOWLEDGEMENTS

We thank Banker lab members for generously providing primary rat hippocampus neuronal cultures. We thank Barbara Smoody and Stefanie Kaech Petrie for their help with neuronal cultures. We thank David Ron and Laurie Glimcher for providing CHOP and XBP1 knock-out MEFs, respectively. We thank Ron Prywes for the 3xFLAG-ATF6 plasmid. We thank members of the Johnson lab for various reagents and members of the Nelson lab for useful discussions. We thank Shailaja Sopory for technical assistance.

This project has been funded in whole or in part with Federal funds from the National Institute of Allergy and Infectious Diseases, National Institutes of Health, Department of Health and Human Services, under contract HHSN266200500027C, and by NIH grant AI 61527 (J.A.N.) and U54 AI57158 (Northeast Biodefense Center [W.I.L.]).

REFERENCES

1. **Agamanolis, D. P., M. J. Leslie, E. A. Caveny, J. Guarner, W. J. Shieh, and S. R. Zaki.** 2003. Neuropathological findings in West Nile virus encephalitis: a case report. Ann. Neurol. **54:**547–551.

1a. **Applied Biosystems.** 1997. User bulletin 2. Applied Biosystems, Foster City, CA.

2. **Briese, T., W. G. Glass, and W. I. Lipkin.** 2000. Detection of West Nile virus sequences in cerebrospinal fluid. Lancet **355:**1614–1615.
3. **Calfon, M., H. Zeng, F. Urano, J. H. Till, S. R. Hubbard, H. P. Harding, S. G. Clark, and D. Ron.** 2002. IRE1 couples endoplasmic reticulum load to secretory capacity by processing the XBP-1 mRNA. Nature **415:**92–96.
4. **Chan, S. W., and P. A. Egan.** 2005. Hepatitis C virus envelope proteins regulate CHOP via induction of the unfolded protein response. FASEB J. **19:**1510–1512.
5. **Chen, X., J. Shen, and R. Prywes.** 2002. The luminal domain of ATF6 senses endoplasmic reticulum (ER) stress and causes translocation of ATF6 from the ER to the Golgi. J. Biol. Chem. **277:**13045–13052.
6. **Davis, L. E., R. DeBiasi, D. E. Goade, K. Y. Haaland, J. A. Harrington, J. B. Harnar, S. A. Pergam, M. K. King, B. K. DeMasters, and K. L. Tyler.** 2006. West Nile virus neuroinvasive disease. Ann. Neurol. **60:**286–300.
7. **Davis, R. J.** 2000. Signal transduction by the JNK group of MAP kinases. Cell **103:**239–252.
8. **de Haro, C., R. Mendez, and J. Santoyo.** 1996. The eIF-2alpha kinases and the control of protein synthesis. FASEB J. **10:**1378–1387.
9. **Dimcheff, D. E., S. Askovic, A. H. Baker, C. Johnson-Fowler, and J. L. Portis.** 2003. Endoplasmic reticulum stress is a determinant of retrovirus-induced spongiform neurodegeneration. J. Virol. **77:**12617–12629.
10. **Fayzulin, R., F. Scholle, O. Petrakova, I. Frolov, and P. W. Mason.** 2006. Evaluation of replicative capacity and genetic stability of West Nile virus replicons using highly efficient packaging cell lines. Virology **351:**196–209.
11. **Guarner, J., W.-J. Shieh, S. Hunter, C. D. Paddock, T. Morken, G. L. Campbell, A. A. Marfin, and S. R. Zaki.** 2004. Clinicopathologic study and laboratory diagnosis of 23 cases with West Nile virus encephalomyelitis. Hum. Pathol. **35:**983–990.
12. **Harding, H. P., M. Calfon, F. Urano, I. Novoa, and D. Ron.** 2002. Transcriptional and translational control in the mammalian unfolded protein response. Annu. Rev. Cell Dev. Biol. **18:**575–599.
13. **Harding, H. P., Y. Zhang, and D. Ron.** 1999. Protein translation and folding are coupled by an endoplasmic-reticulum-resident kinase. Nature **397:**271–274.
14. **He, B., M. Gross, and B. Roizman.** 1997. The gamma(1)34.5 protein of herpes simplex virus 1 complexes with protein phosphatase 1alpha to dephosphorylate the alpha subunit of the eukaryotic translation initiation factor 2 and preclude the shutoff of protein synthesis by double-stranded RNA-activated protein kinase. Proc. Natl. Acad. Sci. USA **94:**843–848.
15. **Hirsch, A. J., G. R. Medigeshi, H. L. Meyers, V. DeFilippis, K. Fruh, T. Briese, W. I. Lipkin, and J. A. Nelson.** 2005. The Src family kinase c-Yes is required for maturation of West Nile virus particles. J. Virol. **79:**11943–11951.
16. **Hong, M., M. Li, C. Mao, and A. S. Lee.** 2004. Endoplasmic reticulum stress triggers an acute proteasome-dependent degradation of ATF6. J. Cell Biochem. **92:**723–732.
17. **Jordan, R., L. Wang, T. M. Graczyk, T. M. Block, and P. R. Romano.** 2002. Replication of a cytopathic strain of bovine viral diarrhea virus activates PERK and induces endoplasmic reticulum stress-mediated apoptosis of MDBK cells. J. Virol. **76:**9588–9599.
18. **Kaech, S., and G. Banker.** 2006. Culturing hippocampal neurons. Nat. Protoc. **1:**2406–2415.
19. **Kazemi, S., S. Papadopoulou, S. Li, Q. Su, S. Wang, A. Yoshimura, G. Matlashewski, T. E. Dever, and A. E. Koromilas.** 2004. Control of alpha subunit of eukaryotic translation initiation factor 2 (eIF2 alpha) phosphorylation by the human papillomavirus type 18 E6 oncoprotein: implications for eIF2 alpha-dependent gene expression and cell death. Mol. Cell. Biol. **24:**3415–3429.
20. **Kojima, E., A. Takeuchi, M. Haneda, A. Yagi, T. Hasegawa, K. Yamaki, K. Takeda, S. Akira, K. Shimokata, and K. Isobe.** 2003. The function of GADD34 is a recovery from a shutoff of protein synthesis induced by ER stress: elucidation by GADD34-deficient mice. FASEB J. **17:**1573–1575.
21. **Kramer, L. D., J. Li, and P. Y. Shi.** 2007. West Nile virus. Lancet Neurol. **6:**171–181.
22. **Kumar, R., S. Azam, J. M. Sullivan, C. Owen, D. R. Cavener, P. Zhang, D. Ron, H. P. Harding, J. J. Chen, A. Han, B. C. White, G. S. Krause, and D. J. DeGracia.** 2001. Brain ischemia and reperfusion activates the eukaryotic initiation factor 2alpha kinase, PERK. J. Neurochem. **77:**1418–1421.
23. **Lazebnik, Y. A., S. H. Kaufmann, S. Desnoyers, G. G. Poirier, and W. C. Earnshaw.** 1994. Cleavage of poly(ADP-ribose) polymerase by a proteinase with properties like ICE. Nature **371:**346–347.
24. **Lee, A. H., N. N. Iwakoshi, and L. H. Glimcher.** 2003. XBP-1 regulates a subset of endoplasmic reticulum resident chaperone genes in the unfolded protein response. Mol. Cell. Biol. **23:**7448–7459.
25. **Lee, K., W. Tirasophon, X. Shen, M. Michalak, R. Prywes, T. Okada, H. Yoshida, K. Mori, and R. J. Kaufman.** 2002. IRE1-mediated unconventional mRNA splicing and S2P-mediated ATF6 cleavage merge to regulate XBP1 in signaling the unfolded protein response. Genes Dev. **16:**452–466.
26. **Li, X. D., H. Lankinen, N. Putkuri, O. Vapalahti, and A. Vaheri.** 2005. Tula hantavirus triggers pro-apoptotic signals of ER stress in Vero E6 cells. Virology **333:**180–189.
27. **Liu, N., V. L. Scofield, W. Qiang, M. Yan, X. Kuang, and P. K. Wong.** 2006. Interaction between endoplasmic reticulum stress and caspase 8 activation in retrovirus MoMuLV-ts1-infected astrocytes. Virology **348:**398–405.
28. **Ma, Y., J. W. Brewer, J. A. Diehl, and L. M. Hendershot.** 2002. Two distinct stress signaling pathways converge upon the CHOP promoter during the mammalian unfolded protein response. J. Mol. Biol. **318:**1351–1365.
29. **Marciniak, S. J., and D. Ron.** 2006. Endoplasmic reticulum stress signaling in disease. Physiol. Rev. **86:**1133–1149.
30. **Marciniak, S. J., C. Y. Yun, S. Oyadomari, I. Novoa, Y. Zhang, R. Jungreis, K. Nagata, H. P. Harding, and D. Ron.** 2004. CHOP induces death by promoting protein synthesis and oxidation in the stressed endoplasmic reticulum. Genes Dev. **18:**3066–3077.
31. **McCullough, K. D., J. L. Martindale, L. O. Klotz, T. Y. Aw, and N. J. Holbrook.** 2001. Gadd153 sensitizes cells to endoplasmic reticulum stress by down-regulating Bcl2 and perturbing the cellular redox state. Mol. Cell. Biol. **21:**1249–1259.
32. **Nanua, S., and F. K. Yoshimura.** 2004. Mink epithelial cell killing by pathogenic murine leukemia viruses involves endoplasmic reticulum stress. J. Virol. **78:**12071–12074.
33. **Nishitoh, H., A. Matsuzawa, K. Tobiume, K. Saegusa, K. Takeda, K. Inoue, S. Hori, A. Kakizuka, and H. Ichijo.** 2002. ASK1 is essential for endoplasmic reticulum stress-induced neuronal cell death triggered by expanded polyglutamine repeats. Genes Dev. **16:**1345–1355.
34. **Novoa, I., H. Zeng, H. P. Harding, and D. Ron.** 2001. Feedback inhibition of the unfolded protein response by GADD34-mediated dephosphorylation of eIF2alpha. J. Cell Biol. **153:**1011–1022.
35. **Oyadomari, S., and M. Mori.** 2004. Roles of CHOP/GADD153 in endoplasmic reticulum stress. Cell Death Differ. **11:**381–389.
36. **Paschen, W., C. Gissel, T. Linden, S. Althausen, and J. Doutheil.** 1998. Activation of gadd153 expression through transient cerebral ischemia: evidence that ischemia causes endoplasmic reticulum dysfunction. Brain Res. Mol. Brain Res. **60:**115–122.
37. **Pavio, N., P. R. Romano, T. M. Graczyk, S. M. Feinstone, and D. R. Taylor.** 2003. Protein synthesis and endoplasmic reticulum stress can be modulated by the hepatitis C virus envelope protein E2 through the eukaryotic initiation factor 2alpha kinase PERK. J. Virol. **77:**3578–3585.
38. **Sampson, B. A., and V. Armbrustmacher.** 2001. West Nile encephalitis: the neuropathology of four fatalities. Ann. N. Y. Acad. Sci. **951:**172–178.
39. **Sampson, B. A., H. Nields, V. Armbrustmacher, and D. S. Asnis.** 2003. Muscle weakness in West Nile encephalitis is due to destruction of motor neurons. Hum. Pathol. **34:**628–629.
40. **Samuel, M. A., and M. S. Diamond.** 2006. Pathogenesis of West Nile virus infection: a balance between virulence, innate and adaptive immunity, and viral evasion. J. Virol. **80:**9349–9360.
41. **Samuel, M. A., J. D. Morrey, and M. S. Diamond.** 2007. Caspase 3-dependent cell death of neurons contributes to the pathogenesis of West Nile virus encephalitis. J. Virol. **81:**2614–2623.
42. **Schroder, M., and R. J. Kaufman.** 2005. The mammalian unfolded protein response. Annu. Rev. Biochem. **74:**739–789.
43. **Shen, J., X. Chen, L. Hendershot, and R. Prywes.** 2002. ER stress regulation of ATF6 localization by dissociation of BiP/GRP78 binding and unmasking of Golgi localization signals. Dev. Cell **3:**99–111.
44. **Shi, P. Y., M. Tilgner, M. K. Lo, K. A. Kent, and K. A. Bernard.** 2002. Infectious cDNA clone of the epidemic West Nile virus from New York City. J. Virol. **76:**5847–5856.
45. **Shrestha, B., D. Gottlieb, and M. S. Diamond.** 2003. Infection and injury of neurons by West Nile encephalitis virus. J. Virol. **77:**13203–13213.
46. **Su, H. L., C. L. Liao, and Y. L. Lin.** 2002. Japanese encephalitis virus infection initiates endoplasmic reticulum stress and an unfolded protein response. J. Virol. **76:**4162–4171.
47. **Szegezdi, E., S. E. Logue, A. M. Gorman, and A. Samali.** 2006. Mediators of endoplasmic reticulum stress-induced apoptosis. EMBO Rep. **7:**880–885.
48. **Tardif, K. D., K. Mori, R. J. Kaufman, and A. Siddiqui.** 2004. Hepatitis C virus suppresses the IRE1-XBP1 pathway of the unfolded protein response. J. Biol. Chem. **279:**17158–17164.
49. **Tardif, K. D., K. Mori, and A. Siddiqui.** 2002. Hepatitis C virus subgenomic replicons induce endoplasmic reticulum stress activating an intracellular signaling pathway. J. Virol. **76:**7453–7459.
50. **Tardif, K. D., G. Waris, and A. Siddiqui.** 2005. Hepatitis C virus, ER stress, and oxidative stress. Trends Microbiol. **13:**159–163.
51. **Tessitore, A., M. del P. Martin, R. Sano, Y. Ma, L. Mann, A. Ingrassia, E. D. Laywell, D. A. Steindler, L. M. Hendershot, and A. d'Azzo.** 2004. GM1-ganglioside-mediated activation of the unfolded protein response causes neuronal death in a neurodegenerative gangliosidosis. Mol. Cell **15:**753–766.
52. **Travers, K. J., C. K. Patil, L. Wodicka, D. J. Lockhart, J. S. Weissman, and P. Walter.** 2000. Functional and genomic analyses reveal an essential coordination between the unfolded protein response and ER-associated degradation. Cell **101:**249–258.
53. **Urano, F., X. Wang, A. Bertolotti, Y. Zhang, P. Chung, H. P. Harding, and D. Ron.** 2000. Coupling of stress in the ER to activation of JNK protein kinases by transmembrane protein kinase IRE1. Science **287:**664–666.
54. **Wang, X. Z., M. Kuroda, J. Sok, N. Batchvarova, R. Kimmel, P. Chung, H.**

Zinszner, and D. Ron. 1998. Identification of novel stress-induced genes downstream of chop. EMBO J. **17:**3619–3630.
55. **Williams, B. L., and W. I. Lipkin.** 2006. Endoplasmic reticulum stress and neurodegeneration in rats neonatally infected with Borna disease virus. J. Virol. **80:**8613–8626.
56. **Xiao, S. Y., H. Guzman, H. Zhang, A. P. Travassos da Rosa, and R. B. Tesh.** 2001. West Nile virus infection in the golden hamster (Mesocricetus auratus): a model for West Nile encephalitis. Emerg. Infect. Dis. **7:**714–721.
57. **Ye, J., R. B. Rawson, R. Komuro, X. Chen, U. P. Dave, R. Prywes, M. S. Brown, and J. L. Goldstein.** 2000. ER stress induces cleavage of membrane-bound ATF6 by the same proteases that process SREBPs. Mol. Cell **6:**1355–1364.
58. **Yoneda, T., K. Imaizumi, K. Oono, D. Yui, F. Gomi, T. Katayama, and M. Tohyama.** 2001. Activation of caspase-12, an endoplastic reticulum (ER) resident caspase, through tumor necrosis factor receptor-associated factor 2-dependent mechanism in response to the ER stress. J. Biol. Chem. **276:** 13935–13940.
59. **Yoshida, H., T. Matsui, N. Hosokawa, R. J. Kaufman, K. Nagata, and K. Mori.** 2003. A time-dependent phase shift in the mammalian unfolded protein response. Dev. Cell **4:**265–271.
60. **Yoshida, H., T. Matsui, A. Yamamoto, T. Okada, and K. Mori.** 2001. XBP1 mRNA is induced by ATF6 and spliced by IRE1 in response to ER stress to produce a highly active transcription factor. Cell **107:**881–891.
61. **Yu, C. Y., Y. W. Hsu, C. L. Liao, and Y. L. Lin.** 2006. Flavivirus infection activates the XBP1 pathway of the unfolded protein response to cope with endoplasmic reticulum stress. J. Virol. **80:**11868–11880.
62. **Zhao, L., and S. L. Ackerman.** 2006. Endoplasmic reticulum stress in health and disease. Curr. Opin. Cell Biol. **18:**444–452.
63. **Zinszner, H., M. Kuroda, X. Wang, N. Batchvarova, R. T. Lightfoot, H. Remotti, J. L. Stevens, and D. Ron.** 1998. CHOP is implicated in programmed cell death in response to impaired function of the endoplasmic reticulum. Genes Dev. **12:**982–995.